

Experiments on wave breaking in stratified flow over obstacles

By IAN P. CASTRO¹ AND WILLIAM H. SNYDER^{2†}

¹Mechanical Engineering Department, University of Surrey, Guildford, Surrey, GU2 5XH, UK

²Atmospheric Sciences Modeling Division, Air Resources Laboratory, National Oceanic and Atmospheric Administration, Research Triangle Park, NC 27711, USA

(Received 19 October 1992 and in revised form 13 April 1993)

Towing-tank experiments on linearly stratified flow over three-dimensional obstacles of various shapes are described. Particular emphasis is given to the parameter regimes which lead to wave breaking aloft, the most important of which is the Froude number defined by $F_h = U/Nh$, where U , N and h are the flow speed, the Brunt–Väisälä frequency and the hill height, respectively. The effects of other parameters, principally $K (= ND/\pi U)$, where D is the fluid depth) and the spanwise and longitudinal aspect ratios of the hill, on wave breaking are also demonstrated. It is shown that the Froude-number range over which wave breaking occurs is generally much more restricted than the predictions of linear (hydrostatic) theories would suggest; nonlinear (Long's model) theories are in somewhat closer agreement with experiment. The results also show that a breaking wave aloft can exist separately from a further recirculating region downstream of the hill under the second lee wave, but that under certain circumstances these can interact to form a massive turbulent zone whose height is much greater than h . Previous theories only give estimates for the *upper* critical F_h , below which breaking occurs; the experiments also reveal *lower* critical values, below which there is no wave breaking.

1. Introduction

It is well known that uniformly stratified flow over obstacles can lead to stationary lee waves which under certain circumstances can break, generating regions of intense turbulence and, sometimes, considerable increase in drag. Such flows have been clearly seen experimentally, both in the field and in the laboratory, and also in some numerical studies. There are currently no complete analytical theories that are able to deal with flows that include wave-breaking regions. In one of the more recent reviews of research on airflow over mountains, Smith (1989*a*) points out that the mountain geometries and upstream stratification parameters that lead to stagnation, either on the hill surface or aloft, are not yet well delineated. Apart from his own extension of linear, hydrostatic theory to the three-dimensional case (elliptical hills of specified shape) nearly all the published values of critical Froude number for which vertical streamlines first occur have been derived from non-linear calculations for two-dimensional obstacles of various shapes (using Long's model, e.g. Long 1953). Thus Huppert & Miles (1969), for example, showed that for flows unbounded above, Long's model for uniformly stratified flow over a semi-ellipse predicts overturning when F_{hc} falls below 1.49, in the hydrostatic limit of a very long ellipse. Here, F_{hc} is the Froude number ($= U/Nh$, where

† On assignment to the Atmospheric Research and Exposure Assessment Laboratory, US Environmental Protection Agency, Research Triangle Park, NC 27711, USA.

U is the upstream velocity, h is the obstacle height and N is the Brunt–Väisälä frequency, $[(-g/\rho_0)\partial\rho/\partial z]^{\frac{1}{2}}$, and the suffix c refers to the critical value at which vertical streamlines first appear, with F_h decreasing. For the other extreme of body shape – a normal flat plate – they found $F_{hc} = 0.58$. Likewise, they found that for a ‘Witch of Agnesi’ body, i.e. one whose height is specified by $n = 1$ in:

$$h(x) = h_m/[1 + (x/a_x)^2]^n, \quad (1)$$

where h_m is the maximum body height, the result for $h_m \rightarrow 0$ is $F_{hc} = 1.18$ (Miles & Huppert 1969). Smith (1989*b*) found, using a linear, hydrostatic theory that if $n = \frac{3}{2}$ then $F_{hc} = 1.72$. And, to quote an early example of a numerical approach, Lilly & Klemp (1979) found that for a continuous sequence of sine-shaped hills $F_{hc} = 0.75$. They were perhaps the first authors to show, using a numerical method, that the critical Froude number depends significantly on the particular cross-sectional shape of the hill.

In the case of three-dimensional obstacles, it is known that F_{hc} depends on the spanwise extent of the obstacle. Linear, small-perturbation theory showed long ago that, for a bell-shaped hill, lee-wave amplitudes increase as the spanwise aspect ratio (width/height) increases (e.g. Crapper 1962) and, more recently, similar theoretical considerations have indicated how F_{hc} depends on the spanwise aspect ratio of a hill whose shape is defined by the three-dimensional version of (1) above, with $n = \frac{3}{2}$ (Smith 1986*b*). Of course, linearization becomes locally invalid as stagnation approaches, so the results of such theoretical work can only be a first approximation. This is emphasized by Smith’s rather surprising result that the value of F_{hc} is virtually insensitive to the value of n (for $1 < n < 4$, at least), which seems at odds with implications from the two-dimensional literature noted above. To quote Smith (1989*a*): ‘linear theory estimates are not sufficiently accurate to serve as a foundation for future research’. Laboratory studies have also demonstrated the effect of spanwise aspect ratio. One of our own experiments, for example, showed that for a triangular-shaped obstacle the range of F_h for which wave breaking occurred increases with increasing spanwise aspect ratio (Castro 1987). The results were shown to be qualitatively consistent with linear theory but it was emphasized that the wave-breaking bounds (in terms of the locus of F_{hc} in the F_h /aspect-ratio plane) would depend on the particular hill shape.

Rottman & Smith (1989) have reported a series of nominally two-dimensional experiments designed to test how well numerical simulations (like those of Clark & Peltier 1977; Durran 1986; and Bacmeister & Pierrehumbert 1988) and the nonlinear hydrostatic theory of Smith (1985) compare with real linearly stratified flow over obstacles. In the latter theory a wave-breaking region is assumed to exist and the flow below this region is analysed on the basis of hydraulic ideas. Rottman & Smith were particularly concerned with the possible sensitivity of the downslope winds resulting from wave breaking to violations of the idealized flow assumptions made in the theory. Their work was the first systematic laboratory study of severe downslope winds but no attempt was made to study the effect of hill shape (rather than height) on the range of F_h leading to wave breaking.

The issue of wave breaking is important, at the very least because of its effects on downslope winds (as already noted), surface drag, and the current uncertainties in handling such relatively fine-scale details in atmospheric circulation models. It would therefore clearly be helpful to have a rather better quantitative understanding of the ways in which obstacle shape affects the wave field. This can only come via numerical and/or laboratory experiments. The latter are also needed as part of the validation process for the former. We have therefore undertaken a range of physical experiments,

using a number of different obstacle shapes and spanwise aspect ratios, complementing the initial work on triangular bodies mentioned earlier and the work of Rottman & Smith (1989). The specific intention was to delineate the range of F_h that, for each body, gave rise to wave breaking aloft. This paper presents the results. In all the experiments the fluid was linearly stratified and the mean flow upstream was uniform. Then, assuming that the Reynolds number is sufficiently high that variations in it will be unimportant, the major parameters are (in the case of infinite domain depth) the Froude number, F_h , and geometrical parameters like W/h and L/h , where W and L are the spanwise width and axial length of the hill. In some circumstances it may be more appropriate to consider alternative parameters formed via suitable combinations of these – $F_L = U/NL$, for example, when considering the position of separation in the lee of the hill (see Hunt & Snyder 1980). Note that for general three-dimensional hills many more than two geometrical parameters are needed to specify the shape completely and some may be important. Surface slope, for example, is likely to be dominant in terms of the occurrence of surface flow separation in the lee. However, in this paper we have chosen to concentrate largely on the effect of variations in W/h and L/h , since it is these that seem dominant in affecting wave breaking aloft.

In laboratory experiments there is an additional parameter that may govern the nature of the lee-wave field. The flows are always bounded above the obstacle (by either a solid surface or a free liquid/air interface) so that, defining the flow depth by D , the particular value of $K = ND/\pi U$ can be important unless the obstacle height satisfies $h/D \ll 1$. Long's model solutions for finite-depth cases certainly suggest substantial variations in F_{hc} with h/D , although some limited data obtained by Baines (1977) indicate that such solutions are not realistic; nonetheless, Baines' data show that h/D might be important for $h/D > 0.15$. In comparing the present results with theoretical results like those quoted above, it is therefore important to consider the possible influence of K (or, equivalently for fixed F_h , the obstacle 'blockage' ratio h/D); some experiments were undertaken specifically to assist in this process.

A variety of different hill shapes and orientations were used in the experiments and in each case the Froude number was varied over a wide range, including the range in which wave breaking might be expected to occur. Smith's (1989*b*) three-dimensional result appears to be the only one in the literature that gives F_{hc} as a continuous function of spanwise aspect ratio, so two of the bodies used in the experiment were defined by the three-dimensional equivalent of equation (1) with $n = \frac{3}{2}$, as used by Smith. Other bodies had either lower or greater surface slopes; details are given in §2, along with other pertinent features of the experimental arrangements. In §3 the major experimental results are presented and discussed, and compared with the current theories and numerical experiments. In the final section the results are summarized and the major conclusions drawn.

2. Experimental arrangements

All the experiments were undertaken in the large towing tank at the USEPA Fluid Modeling Facility. Stratification was achieved in the usual way with salt; further details are given in Thompson & Snyder (1976). Initially linear density profiles were generated and then maintained by syphoning off the upper few centimeters after every few tows, although small changes in the density gradient in a region less than half the hill height in thickness were accepted since these did not change the Froude number in the bulk of the flow over the hill. When the upper few centimeters were removed corresponding layers of appropriate density were introduced at the bottom of the tank.

Hill	Height h_m (cm)	Aspect ratio $\alpha = W/L$	$\beta = W/h_m$	L/h_m	W/W_i	Max. slope (deg.)
CCB1	16.1	0.49	4.85	9.9	0.325	24
CCB2	15.8	1.00	4.85	4.85	0.320	24
CCB3	16.1	2.04	9.90	4.85	0.660	24
SM1	10.0	0.33	1.96	5.86	0.082	34
SM2	10.0	1.00	1.96	1.96	0.082	34
SM3	10.0	3.00	5.86	1.96	0.245	34
COS1	10.0	1.00	1.78	1.78	0.074	40
COS2	10.0	2.34	4.18	1.78	0.174	40
COS3	10.0	3.70	6.59	1.78	0.275	40
COS4	10.0	6.40	11.4	1.78	0.475	40

TABLE 1. Geometrical parameters of the hills. Bodies with $\alpha = 1$ are axisymmetric, W and L are the spanwise width and axial length at the half-height points, respectively, and COS4 is the steep hill used by Rottman & Smith (1989). W_i (column 6) is the spanwise width of the tank.

A number of different obstacles were used. Most of these were adaptations of models used in previous studies, but two new models were constructed specifically for this study. These were of the general shape defined by the three-dimensional equivalent of equation (1) with $n = \frac{3}{2}$, i.e.

$$h(x) = h_m/[1 + (x/a_x)^2 + (y/a_y)^2]^{\frac{3}{2}}.$$

(This was the shape used by Smith 1989*a* in his analytical study.) One model was axisymmetric with $h_m = 10$ cm and $a_x = a_y = 12.75$ cm, giving a maximum surface slope of 34° . The other had the same h_m and a_x , but with $a_y/a_x = 3$. A second family of hills had a shape similar to that used in the experiments of Snyder *et al.* (1985), which was an idealized version of Cinder Cone Butte (an isolated hill in Idaho). The axisymmetric version used in those earlier experiments was specified by

$$h(r) = (h_m + c)/[(1 + (r/a_r)^4)] - c, \quad h(r) = 0 \quad \text{for } r > 77.5 \text{ cm},$$

with $h_m = 15.5$ cm, $c = 1$ cm and $a_r = 38.8$ cm. An elongated version was constructed by inserting a central section of the same cross-sectional shape and of length 78.4 cm. Defining the aspect ratio, $\alpha = W/L$, as the ratio of the spanwise width (W) at the half-height point to the axial length (L) at the half-height point gives this latter body an aspect ratio of two, compared with $\alpha = 3$ for the 'Smith' hill described above. The longer hills of both shapes were also used with their long axes parallel to the towing direction, yielding $\alpha = 0.5$ for the elongated Cinder Cone or 0.33 for the 'Smith' hill. A third class of hills used had cross-sectional shapes defined by

$$h(x) = \frac{1}{2}h_m[1 + \cos(\pi x/L)],$$

with $h_m = 10.4$ cm, $L = 18.5$ cm. This gives a maximum slope of 40° and corresponds to the 'steep' hill used by Rottman & Smith (1989). In the latter study the central section was 100 cm in span (W_c) and the two ends were simply the same cross-sectional profile rotated through 180° . In the present study three additional hills of this type were used, having $W_c = 50, 25$ and 0 cm. The third was therefore an axisymmetric case. The hills will henceforth be designated SM (for the 'Smith' hills), CCB (for the Cinder-Cone Butte models) and COS (for the cosine-shaped hills), and are given numbers in order of increasing spanwise aspect ratio, α . Hence the Smith hills, for example, are SM1, SM2 and SM3, with SM2 being the axisymmetric case and SM1 and SM3 the cases with the longer dimension parallel and normal to the flow, respectively. Table 1 gives the salient details of each hill and includes the ratio of hill width to channel

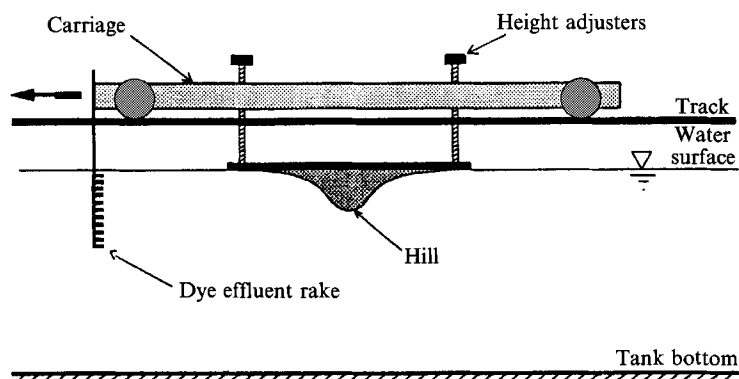


FIGURE 1. General experimental arrangement.

width (W/W_t); the possible influence of this parameter is discussed later. Figure 4(b) shows the mid-span cross-sections of each hill and is included to aid later discussion.

The models were mounted in turn on a baseplate and towed upside down at the water surface with the baseplate immersed by about 5 mm. Details of the arrangements are essentially identical with those of Rottman & Smith (1989); figure 1 shows the general set-up. All discussion is in terms of an inverted laboratory vertical coordinate (i.e. as if the body were the right way up with all flow above its surface). The flow was visualized using dye streamers, which correspond to streamlines in cases where the flow was essentially steady. These were emitted from a rake of tubes well upstream of the model and tailored to ensure that each streamer was neutrally buoyant at its point of release.

Video and still pictures were obtained throughout each tow using cameras mounted at the side of the channel and moving with the carriage. The number of streamers and their locations were varied to suit the anticipated flow in each case, with particular care taken to ensure that there were two or more streamers above any wave-breaking region, in addition to a number at lower elevations.

For each hill a series of tows was performed, consisting of a sequence of Froude numbers spanning either the range over which wave breaking occurred or, if it did not, the range within which the wave amplitudes reached their maximum. Most tows were undertaken with a total water depth around 1 m, but a few series used significantly lower depths (80 or 50 cm) in order to assess the influence of the parameter $K (= ND/\pi U)$.

3. Results and discussion

3.1. Wave-breaking regimes

Very many tows were undertaken and it would not be appropriate to present all the resulting photographs. Instead, just a few examples will be given to demonstrate the major features and we will present the essential results in graphical form using data deduced from the flow visualization. Figure 2 shows a set of photographs from the tows using COS3, spanning the F_h -range at which wave breaking first starts (as F_h is reduced) and then stops. Several features are evident. In figure 2(a) ($F_h = 0.8$) it is clear that wave-breaking does not occur aloft, but the flow separates under the first lee-wave crest, leading to a downstream separation zone which almost matches the hill shape. There also seems to be a further separation region underneath the second lee-wave

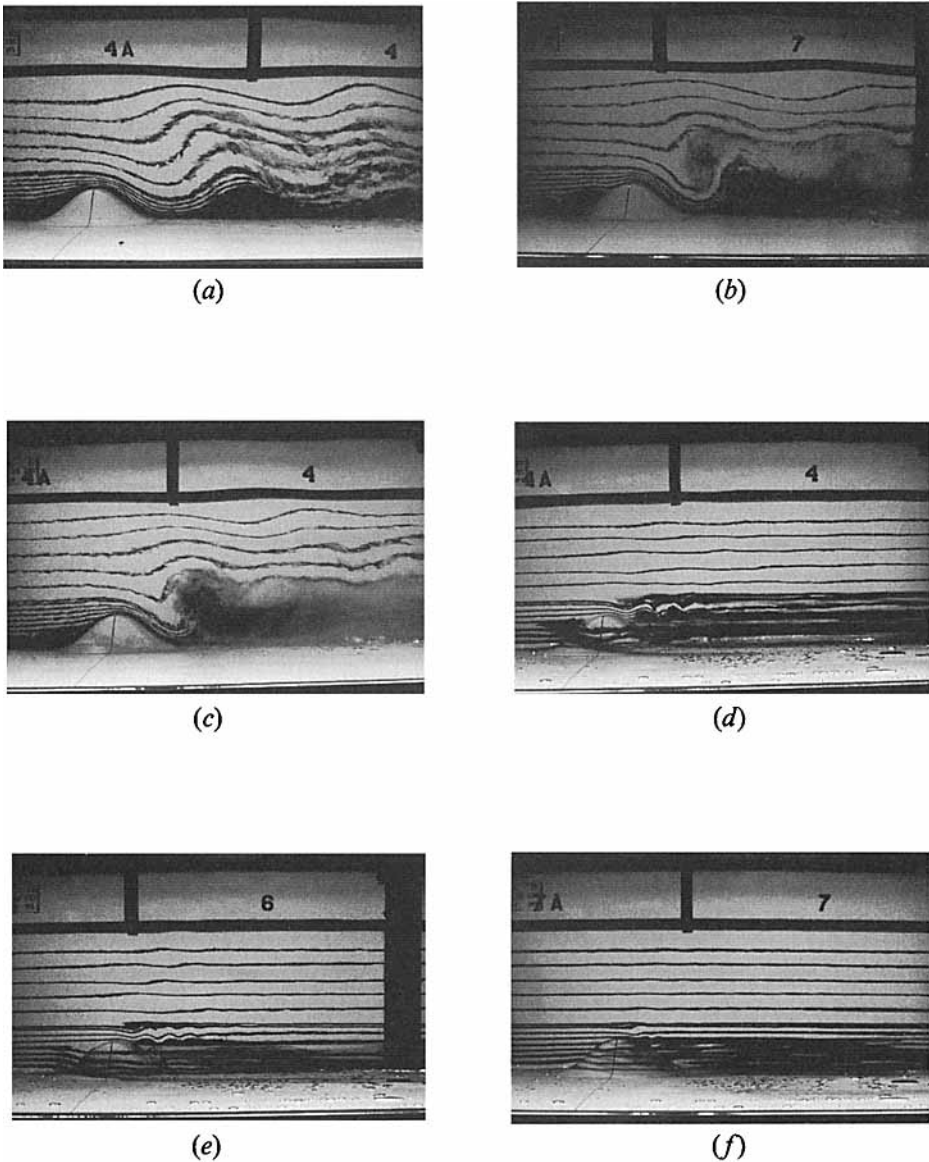


FIGURE 2. Sequence of photographs for the flow over COS3: (a) $F_h = 0.8$; (b) 0.7; (c) 0.6; (d) 0.2; (e) 0.15; (f) 0.1.

crest. In this case K was around 3; for larger D/h (i.e. larger K) the wave amplitude would decay more rapidly with distance downstream, so this region would perhaps disappear. Note that there is no separation from the lee of the hill itself; the later separation (occurring at about $x = \frac{1}{2}\lambda$ where λ is the wavelength ($2\pi F_h h$) and x is measured from the hill crest) is controlled by the lee-wave field, not by the Reynolds number, which ranged from about 1300 at the lowest F_h and smallest hills to about 20000 at the highest F_h . Hunt & Snyder (1980) give a more detailed discussion of the circumstances that lead to surface separation. As F_h is reduced the wavelength falls so that the downstream separation region moves nearer to the hill (figure 2 b, $F_h = 0.7$). Simultaneously the waves steepen and break, so that there is a clear breaking region

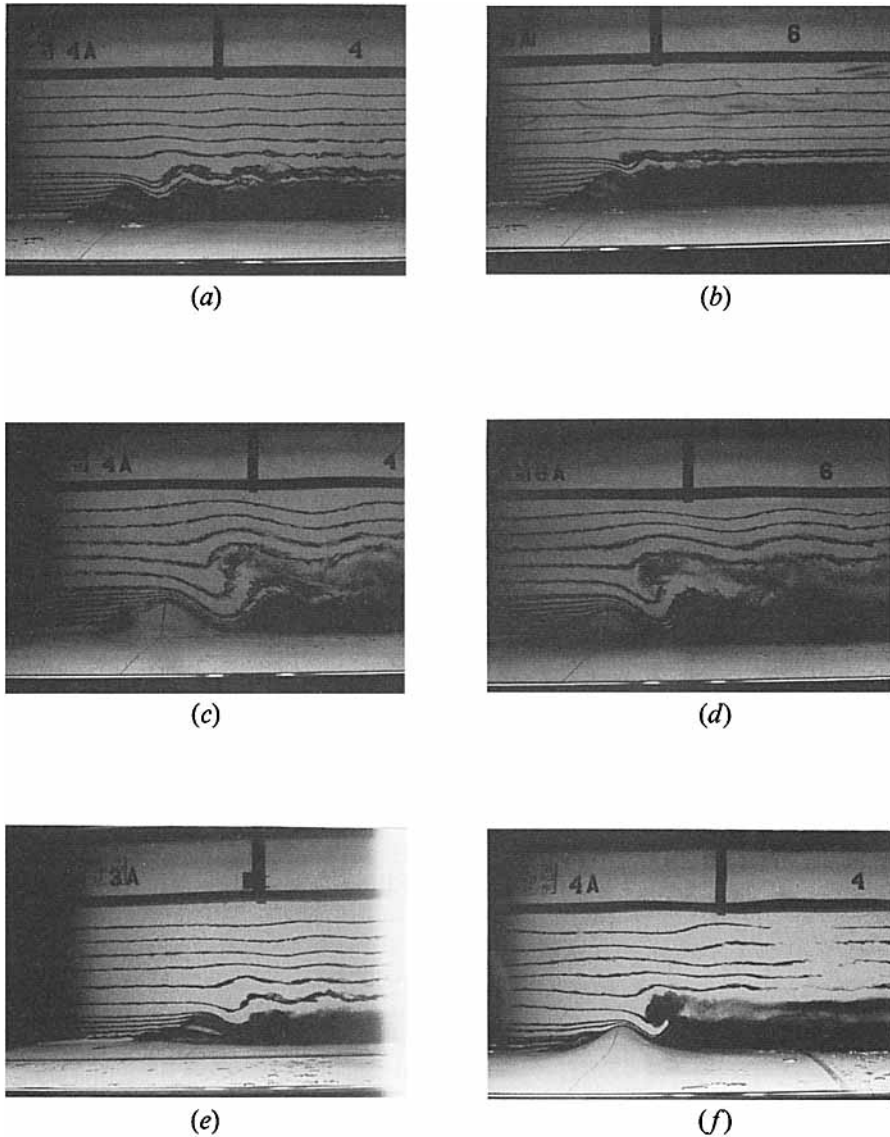


FIGURE 3. Sequence of photographs for the flow over COS1: (a) $F_h = 0.4$, (b) 0.3; COS2: (c) $F_h = 0.7$, (d) 0.6; SM2: (e) $F_h = 0.4$; SM3: (f) 0.4.

aloft, which remains quite distinct from the separated zone under what would be the lee wave crest if breaking had not occurred. In circumstances where wave breaking occurred this distinction between the breaking region and a surface separation region was a common, but not universal, feature of the flow. As the Froude number is reduced further, figure 2(c) ($F_h = 0.6$) shows that these two, previously distinct, turbulent regions merge, leading to what in the past (e.g. Hunt & Snyder 1980) may have been termed an ‘internal hydraulic jump’.

The flows in all these cases were essentially steady throughout the tow. In the corresponding cases (COS4) studied by Rottman & Smith (1989), they found that at $F_h = 0.7$ and 0.8 breaking occurred only intermittently, with the well-mixed region disappearing between each episode of wave breaking. The implication is that in this

case of a somewhat wider hill the flow was, in fact, unsteady at those Froude numbers. Castro, Snyder & Baines (1990) have demonstrated the possibility of periodic unsteadiness in the wave field (and the corresponding surface drag); this most readily occurs for two-dimensional obstacles but wide three-dimensional obstacles can lead to similar behaviour. Indeed, the wide cosine-shaped hill used by Castro *et al.* was marginally less wide than COS4 and yielded noticeably unsteady, periodic drag variations for F_h near 0.7. This point will be discussed further in due course.

Figure 2(*d-f*) shows the flow at the lower end of the Froude-number range. Breaking occurs at $F_h = 0.2$ and perhaps at two different heights at $F_h = 0.15$, but not at all at $F_h = 0.1$. Rottman & Smith (1989) did not study $F_h < 0.2$ but the existence of a lower critical Froude number, below which breaking does not occur, has previously been demonstrated in the case of triangular hills (Castro 1987). It must be said, however, that it was not always easy to decide whether or not breaking occurred at these lowest Froude numbers. At $F_h = 0.1$, for example, the wavelength was significantly less than the hill height, so in some cases wave amplitudes of the same order as the thickness of the dye streamers could have led to unnoticed wave breaking. It is possible that the location (or even existence) of this lower boundary F_{hc} is determined by viscous processes (P. G. Baines, private communication); further work would be necessary to pursue this, but we believe that, whatever the Reynolds number, wave breaking must cease at sufficiently low F_h , since increasingly strong stratification greatly inhibits vertical motions.

For the same (cross-sectional) shape hill, reduction in the spanwise width led to a decrease in the upper critical Froude number. Figure 3 shows examples of the flow fields for COS1, COS2, SM2 and SM3. Note that for COS1, the axisymmetric case, wave breaking *only* occurred at $F_h = 0.3$, in the sequence $F_h = 0.2, 0.3, 0.4$ and 0.5 (cf. figure 3*a, b*) and, for COS2, wave breaking was marginal for $F_h = 0.7$ (figure 3*c*). At $F_h = 0.6$, in contrast to the COS3 result (figure 2*c*), the two recirculating regions remained quite distinct (figure 3*d*), even though surface separation occurred around the base of the hill ($x = \frac{1}{2}\lambda = 1.9h$). Maintaining the aspect ratio but reducing the hill slope also sometimes led to a reduction in the (upper) critical Froude number. SM3, having a surface slope of 34° and an aspect ratio of $\alpha = 3$, generated wave breaking but over a smaller Froude-number range than COS3, which had a slope of 40° , despite the fact that COS3 had a rather lower α (2.34). However, this trend was not universal, as discussed later. Figures 3(*e*) and 3(*f*) compare the flow fields for SM2 and SM3 at $F_h = 0.4$, emphasizing the fact that as the spanwise aspect ratio increased wave amplitudes also increased.

These and all the other results are summarized in figure 4(*a*), where the critical Froude number is plotted for each hill shape as a function of aspect ratio. In each case the symbols mark Froude numbers for which wave breaking definitely occurred and the vertical bars drawn from the symbols cover the range of uncertainty, within which wave breaking *may* occur. Sometimes these simply extend halfway to the next F_h value tested, if at that F_h breaking clearly did not occur. Otherwise they are longer, denoting that at the next F_h in the sequence breaking occurred either late in the tow (where wave reflections may have become influential), or earlier in the tow before disappearing later. Points corresponding to Rottman & Smith's (1989) COS4 results are included in the figure, along with the data previously obtained for a triangular ridge (Castro 1987), and smooth curves are drawn through the data as an aid to clarity. Despite the inevitable uncertainties over precisely when steady wave breaking sets in, it is clear that each obstacle shape (shown in figure 4*b*) generates its own 'envelope', within which breaking occurs.

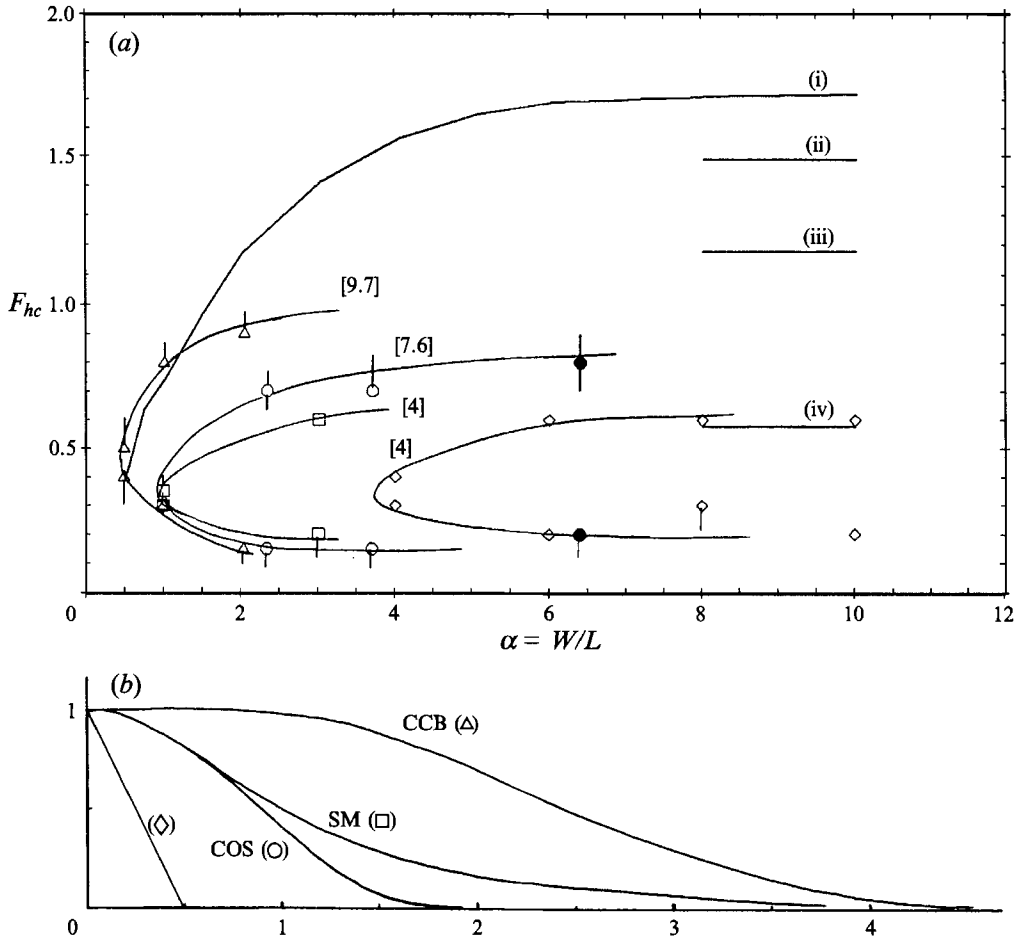


FIGURE 4. (a) Variation of critical Froude number with aspect ratio. Δ , CCB; \circ , COS; \square , SM; \diamond , triangular bodies (Castro 1987). \bullet , COS4 (Rottman & Smith 1989). Figures in square brackets denote values of $\beta = W/h_m$ at $\alpha = 4$. Lines through data points are for clarity only. Solid line (i) is three-dimensional theory from Smith (1989*b*); (ii) Miles & Huppert (1969), ellipse (hydraulic limit); (iii) Huppert & Miles (1969), Agnesi hill; (iv) Miles & Huppert (1969), flat plate. Lines (ii–iv) are for two-dimensional, $\alpha = \infty$, cases. (b) Hill shapes, to scale with distances normalized by hill height. Symbols refer to those used in (a).

An immediate point to emphasize from figure 4(a) is that the trend of increasing envelope area (wider wave breaking F_h range at given α) is not generally monotonic with hill slope, despite the example mentioned earlier. Indeed, the hills with the lowest slope (CCB) are the most susceptible to wave breaking. However, the trend *is* monotonic with increasing aspect ratio, β , if the latter is defined as spanwise width/hill height (W/h_m). To make this clear, the values of β appropriate to each hill at a particular value of α ($\alpha = 4$) are included as bracketed values on the figure. Note that for the triangular hill at $\alpha = 4$, $\beta = 4$ just as for the SM hill at the same α , but wave breaking occurs over a much smaller range of F_h . However, separation occurred at the top of the triangular hill and there was a large recirculation region downwind, so that the *effective* α (considering this region as an extension of the length, L , of the body) is less than the geometrical value used in figure 4(a). The data show that as β increases, the wave-breaking range increases for a given α and this trend would seem to be

independent of hill slope. This is not surprising, since a particular hill slope is not linked directly with the spanwise width, except for axisymmetric hills. Emphasis on hill slope can therefore be misleading and, in considering wave-breaking bounds in practical cases, it is much more important to know α and β (W/L and W/h_m).

A further point to note from figure 4(a) is that any changes in the lower critical Froude number with hill shape, or indeed with α for $\alpha > 4$, are not discernable above the experimental uncertainties (except in the case of the triangular hills, which are anyway somewhat anomalous because of the relatively large separation zones, as indicated above). This is, perhaps, not surprising; in the limit of zero F_h the flow around three-dimensional obstacles occurs in horizontal planes, is effectively decoupled from the flow above, and depends on W only via its effect on the Reynolds number, WU/ν . The lower critical F_h is almost uniformly in the range 0.1–0.2.

It is pertinent to ask at this point whether these general results are likely to be affected by the inevitable flow constriction caused by the tank sidewalls. This is clearly more likely to be the case for the larger W/W_t values and in cases of very low F_h , when the flow is more constrained to move horizontally. One would expect sidewall influence to be qualitatively equivalent to an increase in spanwise width of the hill – forcing more flow over rather than around the hill. This would presumably lead to larger wave amplitudes and an increase in F_{hc} . It is instructive to consider the results for the two cases of largest W/W_t – CCB3 and COS4 (see table 1). Figure 4(a) shows that in these two cases there is no sudden increase in F_{hc} and, if the effect increases with W/W_t (which it must) and is significant, the true (infinite W_t) locus of the F_{hc} boundary would be somewhat lower and flatter than the results indicate. This may be the case but the effect is unlikely to remove the significant differences between the different hill shapes, nor the differences between experiment (for the Smith hills) and the linear theory. Indeed, it would *increase* the latter.

All the cases discussed thus far used a nominal water depth, D , of 1 m, so that the hill height was only $0.1D$ ($0.15D$ in the case of the CCB hills). Whilst this might be thought sufficiently small to imply only weak effects from the upper boundary, it should be noted that $h = 0.1D$ implies $K = ND/\pi U = 3.2$ at $F_h = 1.0$, so that only a relatively small number ($\text{Int}(K)$) of discrete wave modes can exist. Further, since $K > 1$ for all the experiments, upstream wave motions can occur, although they will generally be weak in view of the three-dimensional nature of the hills (Castro & Snyder 1990). In addition, most of the theoretical work has considered the infinite-depth case, so a few further tests (with smaller water depths) were undertaken to assess the influence of h/D . These used the CCB3 and the COS2 hills and figure 5 summarizes the results. Over the range of h/D for which data are available, the changes in F_{hc} are not large, but they could be interpreted as implying rather larger changes for small h/D ($h/D < 0.1$). However, this would be at variance with the deductions of Baines (1977) – his data for F_{hc} as a function of h/D in the case of a ‘Witch of Agnesi’ hill are included. These were deduced from his $\pi h/D$ vs. K plot of the stability boundary derived from a very limited number of data points (Baines’ figure 1). The results do not at first sight seem consistent with the present data, since it is difficult to see why flow over the Agnesi hill should be so much more sensitive to h/D (once $h/D > 0.15$) than that over our CCB3 or COS2 hills. However, Baines’ hill was *two-dimensional* and such ‘blockage’ effects will certainly be greatest in the two-dimensional case. Furthermore, some of the flows may well have been unsteady. Baines’ data do at least agree with the physically plausible argument that changes in F_h with h/D will be smaller at low than at high h/D . We tentatively conclude that F_{hc} values for the infinite-depth case will be no more than about 25% greater than those shown in figure 4(a), for all

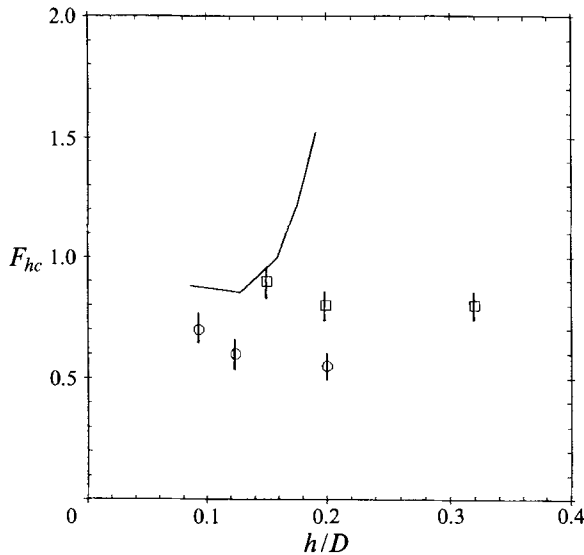


FIGURE 5. Critical Froude number as a function of domain depth. \circ , COS2; \square , CCB3. Solid line is deduced from Baines (1977), for flow over a two-dimensional ‘Agnesi’ hill.

hill shapes. Nonetheless, this effect must be borne in mind when comparing the results with theoretical predictions, and data for $h/D < 0.1$ would certainly be useful. The required experiments would not be easy if the Reynolds number (which falls as h falls) were to be kept sufficiently high to minimize its effects.

3.2. Comparisons with theory

The various analytical and numerical calculations of F_{hc} discussed in §1 are included in figure 4(a). Note first that Smith’s (1989*b*) linear theory predicts F_{hc} larger by a factor of more than two at $\alpha = 2$. In the present experiments no SM hill with $\alpha = 2$ was available, but for $\alpha = 3$ F_{hc} is about 0.6, compared with the 1.4 predicted by the theory. At $\alpha = 1$ breaking occurred over a very limited range between about $F_h = 0.25$ and 0.35, whereas the theory predicts a critical Froude number of about 0.75. The small increases in F_{hc} with decreasing h/D (figure 5) cannot account for this discrepancy and it must be concluded that nonlinear effects lead to a significant reduction in wave amplitudes. This was recognized by Smith, who pointed out that the nonlinear Long’s model for the ‘Witch of Agnesi’ hill with $\alpha = \infty$ gives $F_{hc} = 1.18$ (cf. Smith’s 1.72) and the numerical computation of Smolarkiewicz & Rotunno (1989) for a SM2 hill gave $F_{hc} = 0.56$ (cf. Smith’s 0.75); these values suggest that the linear theory overpredicts F_{hc} by around 30%. Our experiments suggest that the error is even larger.

Whilst there are obvious discrepancies at finite α , figure 4 seems to indicate that the nonlinear theories for $\alpha = \infty$ may represent reasonable asymptotic limits. Despite the fact that the theory cannot account for flow separation behind the obstacle, the flat-plate result for $F_{hc} = 0.58$ is close to the asymptotic trend of the experimental data for the hill most like a flat plate – the triangular bodies used by Castro (1987). As the hill gets longer in the axial direction, the asymptotic F_{hc} certainly rises, as it does in the theory. An alternative way to present the data in figure 4 is to cross-plot it in the form of F_{hc} as a function of L/h_m (an aspect ratio based on *axial* length and hill height). This is done in figure 6 and the results are compared with the results of Huppert & Miles’

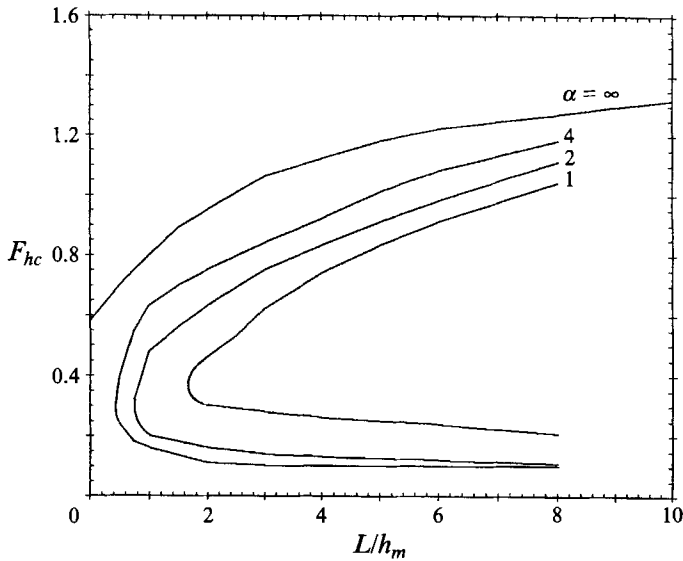


FIGURE 6. Critical Froude number a function of axial aspect ratio, L/h_m . Lines are contours of constant α deduced from the data in figure 4(a), with values of α given on the right. The $\alpha = \infty$ line is the Huppert & Miles (1969) result for an elliptical hill.

(1969) nonlinear (two-dimensional) analysis for an elliptical hill. We have chosen to plot the data as contours of constant α ; the theoretical results correspond to $\alpha = \infty$. For $\alpha < \infty$ the contours are deduced from smoothed curves drawn through the experimental data points shown in figure 4. The nonlinear theory does seem to provide a reasonable asymptotic ($\alpha = \infty$) upper bound on the critical Froude numbers.

It must be emphasized that if the hill is wide enough in the spanwise direction ($\alpha > 4$ in the present context) our previous work has demonstrated that the flows are, in fact, unsteady (Castro *et al.* 1990); periodic, roughly sinusoidal variations in wave amplitude and obstacle drag occur on a relatively long timescale. As noted earlier, the COS4 results of Rottman & Smith (1989) also seemed unsteady, as would be expected from this earlier work. This is obviously not a feature that can be captured by (linear or nonlinear) theories based on steady flow equations. However, that it is *not* some artifact of the experimental technique has now been independently demonstrated via time-dependent numerical computations using the full (laminar) Navier–Stokes equations (Paisley & Castro 1992). It has also more recently been shown to occur at high Reynolds numbers, when the computations used a simple turbulence model (M. F. Paisley, private communication) and has been demonstrated in the inviscid calculations of Lamb (1992). Although the precise reasons for these large-amplitude oscillations in the lee-wave structure have not been fully delineated the essential mechanisms involved have been discussed via nonlinear analysis by Grimshaw & Yi (1991), and Hanazaki (1989*a, b*) presented the first detailed numerical study of advancing upstream modes and their (sometimes) unsteady behaviour.

Oscillatory behaviour can occur both with and without the presence of wave breaking – both cases have been seen during some of our previous experiments and have been found in our recent computations (to be separately reported). All the results to date suggest that oscillatory behaviour occurs most strongly when K is (roughly) in the upper half of each integer range – i.e. for $1.5 < K < 2$, etc. The experimental evidence is that the oscillations can still have significant amplitude for $K > 3$ but it is

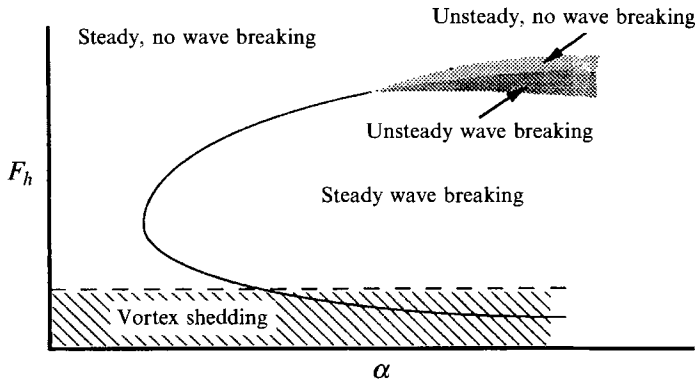


FIGURE 7. Sketch of likely flow regimes, for K sufficiently low to give the possibility of oscillatory behaviour (see text).

not yet clear how rapidly the amplitude of such oscillations falls with increasing K (to $K > O(10)$, say). In figure 7 we indicate qualitatively all the probable flow regimes in the (F_h, α) -plot (cf. figure 5). If the obstacle blockage (h/D) is such that the unsteadiness is very weak or non-existent (for sufficiently large K , presumably) then the stippled regions on figure 7 will disappear.

The sketch also includes the low-Froude-number vortex shedding regime; it is well known that for low F_h (typically below about 0.3) the suppression of vertical motions can lead to large-scale vortex shedding in horizontal planes. This has been discussed in previous papers (Castro, Snyder & Marsh 1983; Castro 1987) and was also evident (but not studied) in the present work. In principle the regime must continue to (but not include) the $\alpha = \infty$ two-dimensional limit, but it is not clearly seen in experiments for the widest three-dimensional hills because the shedding timescales are then of the same order as the tow time. The tank sidewall effects also become significant in such cases. It should be noted that we noticed wave breaking in at least one case where vortex shedding also occurred (the SM2 hill at F_h around 0.3) – hence the overlap of the two regimes in figure 7. However, the two processes may not always be simultaneous, so the sketch is somewhat tentative in this regard.

In addition to being steady state, all theories to date are inviscid, so they cannot capture one of the major features often evident in experiments – separation at the surface under lee-wave crests and a resulting recirculation zone downstream of the hill. Our experiments (and probably earlier ones like those of Hunt & Snyder 1980) show that this separated zone can, in some circumstances, merge with the turbulent, fully mixed zone aloft, caused by wave breaking. This leads to a very deep well-mixed zone which extends all the way to the surface (e.g. figure 2c). Figure 8 shows the variations of H_0 , the upstream height of the streamline that just surmounts the breaking zone, and d_m , the height of the bottom of the wave-breaking region, as a function of F_h for the SM3 and the COS3 hills. Merging does not occur for SM3, so that $d_m > 0$ throughout the wave-breaking range – roughly $0.15 < F_h < 0.65$. However, for COS3 merging does occur – $d_m = 0$ over a small range of F_h near 0.6 – as indicated by the dashed line drawn through the data points. Note that in this case H_0 also falls a little when merging occurs.

A few of these cases of ‘merged’ flow appeared quite like the flow postulated by Smith (1985) in order to use (nonlinear) hydraulic ideas to determine the flow over the lee of the hill. Figure 9 shows two photographs from a tow of the COS4 hill at

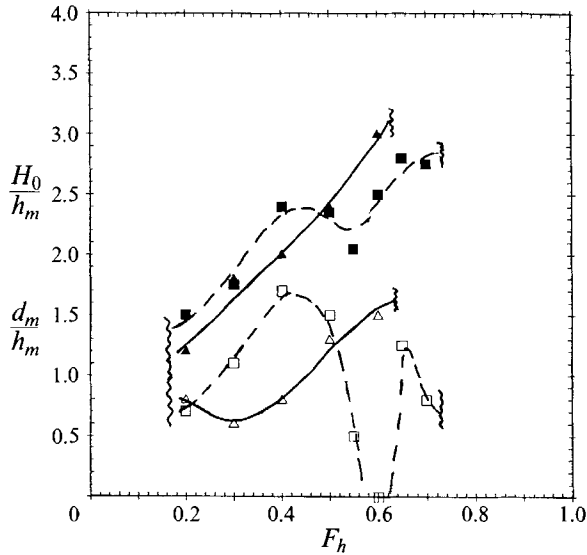


FIGURE 8. Upstream height (H_0 , solid symbols) of the streamline marking the top of the breaking zone, and the height (d_m , open symbols) of the bottom of the breaking zone: triangles, SM3; squares, COS3. Lines added for clarity. The vertical wavy lines mark the limit of the breaking regimes.

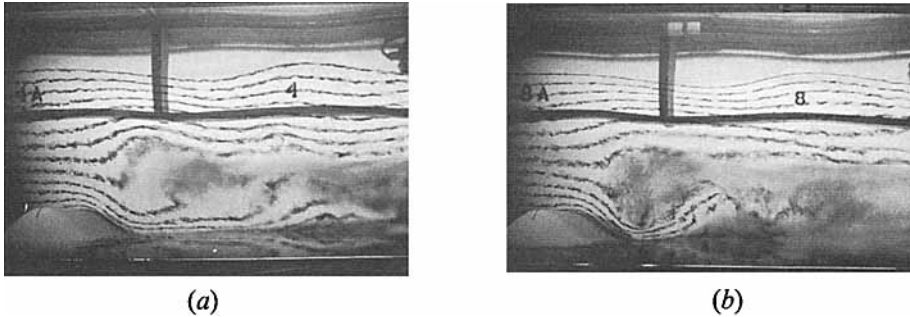


FIGURE 9. Photographs of the flow at two times (t) in a tow of COS4 at $F_h = 0.75$. (a) $t/T = 0.44$; (b) $t/T = 0.56$. T is total tow time.

$F_h = 0.75$. The first (figure 9a), taken about halfway through the tow, shows a well-mixed region whose shape is very similar to the 'triangular wedge' drawn by Smith (e.g. figure 1 of Smith 1985). However, this case was somewhat unsteady; figure 9(b), taken some seconds later, shows a clear separation between the breaking region and a surface separation zone. Nonetheless, Rottman & Smith (1989) concluded that these ideas do seem to lead to reasonable predictions of the height of the upstream streamline that marks the top of the well-mixed region. The present results provide further confirmation of this conclusion, whether or not merging occurs. Figure 10 shows the upstream height for cases SM3 and COS3, normalized by N and U and compared with the results obtained using hydraulic ideas – Smith's (1985) theory as modified by Rottman & Smith (1989). The data display the same level of agreement as found by Rottman & Smith (their figure 6), despite the fact that, in the COS3 case, complete merging of the two well-mixed regions occurs for F_h around 0.6 and the merged region looks rather *less* like Smith's wedge (see figure 2c, cf figure 9a). In Rottman & Smith's

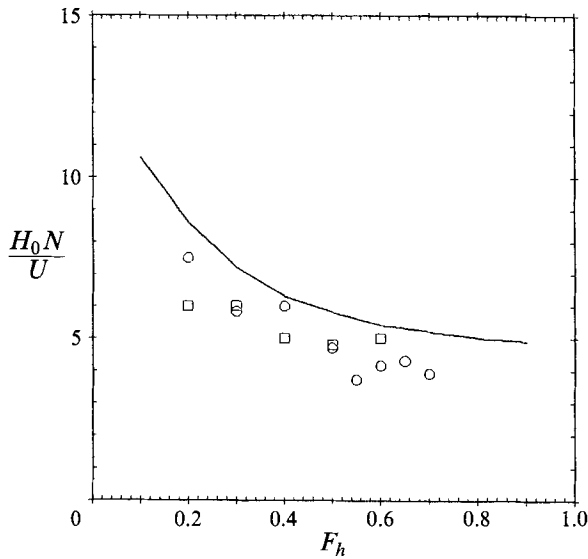


FIGURE 10. Normalized H_0 compared with Smith's theory (solid line). \square , SM3; \circ , COS3.

experiments merging must also have occurred, but they did not discuss the phenomenon. Note also that there are other aspects of the flow that the Smith (1985) theory does not capture very well (see Rottman & Smith 1989).

Finally, we emphasize that linear theory predicts the lee-wave wavelengths very well, although this was not studied in great detail in the present work (but see Castro *et al.* 1983, for example). Note that whenever $\text{Int}(K) > 1$ there is the possibility that a mode with mode number higher than the first (i.e. $n > 1$) will be amplified more by the topography than will the first mode ($n = 1$). Indeed, even linear theory (e.g. Janowitz 1981, 1984; Wong & Kao 1970) suggests that the wave amplitude increases with wavenumber. This has been confirmed (in nonlinear cases) by both experiment (Castro & Snyder 1988) and numerical computation (Hanazaki 1989*b*), at least for the upstream-propagating modes. Presumably the same is true for the lee waves but this is difficult to check since the (stationary) lee waves of different mode number coexist and interact. A referee has suggested that the wave breaking at low F_h (corresponding to $K > 3$, say) is not essentially a mode-1 phenomenon, because higher-order modes have larger amplitudes. This may be correct but, even in these cases, the lee wavelengths in our experiments seemed always to be quite close to those given by linear theory for the first mode. We very rarely saw wave breaking at more than one height, although this would in principle be a possibility for $\text{Int}(K) > 1$.

4. Conclusion

It has been shown, firstly, that linear theory seriously overpredicts the F_h at which wave breaking first occurs, with the implication that non-hydrostatic or nonlinear effects generally act to restrict the range of wave breaking. For bodies sufficiently narrow in the cross-stream direction, wave breaking may not occur for *any* F_h , contrary to some linear theory predictions. Secondly, the condition (in the lee of the obstacle) sometimes referred to as an internal hydraulic jump – e.g. Hunt & Snyder (1980) – seems to occur whenever the wave-breaking region aloft is sufficiently large to ‘merge’ with a separated (rotor) region near the surface. This leads to particularly strong downslope

winds and thence (presumably) to particularly high drag. The range of F_h over which wave breaking occurs is strongly dependent on the shape of the hill, but not primarily on the surface slope. Finally, it has been shown that for all obstacle shapes wave breaking is effectively suppressed at sufficiently small F_h – around 0.1–0.2 for wide hills. If wave breaking does begin at some F_{hc} (with F_h falling), there is therefore always a lower critical F_h at which it ceases. This end of the wave-breaking range does not seem to have been predicted theoretically, although it was noted in our earlier experiment (Castro 1987) and might be expected intuitively.

We are grateful to the staff of the Fluid Modeling Facility, US Environmental Protection Agency, for making this research possible. The diligence of Mr L. Marsh in conducting most of the experiments is particularly acknowledged and we also benefited from useful discussion with Dr Jim Rottman and helpful suggestions from the referees. I.P.C. acknowledges support from North Carolina State University under Cooperative agreements with the US Environmental Protection Agency (nos. CR-814346 & CR-817931), for visits during which the work was undertaken and written up. This paper has been subjected to Agency review and approved for publication. Mention of trade names or commercial products does not constitute endorsement or recommendation for use.

REFERENCES

- BACMEISTER, J. T. & PIERREHUMBERT, R. T. 1988 On high drag states of non-linear stratified flow over an obstacle. *J. Atmos. Sci.* **45**, 63–80.
- BAINES, P. G. 1977 Upstream influence and Long's model in stratified flows. *J. Fluid Mech.* **82**, 147–159.
- CASTRO, I. P. 1987 A note on lee-wave structures in stratified flow over three-dimensional ridges. *Tellus* **39A**, 72–81.
- CASTRO, I. P. & SNYDER, W. H. 1988 Upstream motions in stratified flow. *J. Fluid Mech.* **187**, 487–506.
- CASTRO, I. P. & SNYDER, W. H. 1990 Obstacle drag and upstream motions in stratified flow. In *Stratified Flows* (ed. E. J. List & G. H. Jirka), pp. 84–98. ASCE.
- CASTRO, I. P., SNYDER, W. H. & BAINES, P. G. 1990 Obstacle drag in stratified flow. *Proc. R. Soc. Lond. A* **429**, 119–140.
- CASTRO, I. P., SNYDER, W. H. & MARSH, G. L. 1983 Stratified flow over three-dimensional ridges. *J. Fluid Mech.* **135**, 261–282.
- CLARK, T. L. & PELTIER, W. R. 1977 On the evolution and stability of finite amplitude mountain waves. *J. Atmos. Sci.* **34**, 1715–1730.
- CRAPPER, G. D. 1962 Waves in the lee of a mountain with elliptical contours. *Phil. Trans. R. Soc. Lond. A* **254**, 601.
- DURRAN, D. R. 1986 Another look at downslope windstorms. Part 1: the development of analogs to supercritical flow in an infinitely deep, continuously stratified fluid. *J. Atmos. Sci.* **43**, 2527–2543.
- GRIMSHAW, R. H. J. & YI, Z. 1991 Resonant generation of finite-amplitude waves by the flow of a uniformly stratified fluid over topography. *J. Fluid Mech.* **229**, 603–628.
- HANAZAKI, H. 1989a Drag coefficient and upstream influence in three-dimensional stratified flow of finite depth. *Fluid Dyn Res.* **4**, 317–332.
- HANAZAKI, H. 1989b Upstream advancing columnar disturbances in two-dimensional stratified flow of finite depth. *Phys. Fluids A* **1**, 1976–1987.
- HUNT, J. C. R. & SNYDER, W. H. 1980 Experiments on stably and neutrally stratified flow over a model three-dimensional hill. *J. Fluid Mech.* **96**, 671–704.
- HUPPERT, H. E. & MILES, J. W. 1969 Lee waves in a stratified flow. Part 3. Semi-elliptical obstacle. *J. Fluid Mech.* **35**, 481–496.

- JANOWITZ, G. S. 1981 Stratified flow over a bounded obstacle in a channel of finite depth. *J. Fluid Mech.* **110**, 160–171.
- JANOWITZ, G. S. 1984 Upstream disturbances in stratified channel flow. Unpublished Rep., Dept. of Marine, Earth & Atmospheric Sciences, N.C.State Univ., Raleigh, NC 27650.
- LAMB, K. G. 1992 Inviscid flow over an obstacle: some numerical simulations. Paper presented at 4th IMA Conf. on Stably Stratified Flows, Guildford.
- LILLY, D. K. & KLEMP, J. B. 1979 The effects of terrain shape on non-linear hydrostatic mountain waves. *J. Fluid Mech.* **95**, 241.
- LONG, R. R. 1953 Some aspects of flow of stratified fluids, I: a theoretical investigation. *Tellus* **5**, 42–57.
- MILES, J. W. & HUPPERT, H. E. 1969 Lee waves in a stratified flow. Part 4. Perturbation approximations. *J. Fluid Mech.* **35**, 497–525.
- PAISLEY, M. F. & CASTRO, I. P. 1992 Steady and unsteady computations of strongly stratified flow over two-dimensional obstacles, Paper presented at 4th IMA Conf. on Stably Stratified Flows, Guildford.
- ROTTMAN, J. W. & SMITH, R. B. 1989 A laboratory model of severe downslope winds. *Tellus* **41A**, 401–415.
- SMITH, R. B. 1985 On severe downslope winds. *J. Atmos. Sci.* **42**, 2597–2603.
- SMITH, R. B. 1989a Mountain-induced stagnation points in hydrostatic flow. *Tellus* **41A**, 270–274.
- SMITH, R. B. 1989b Hydrostatic airflow over mountains. *Adv. Geophys.* **31**, 1–41.
- SMOLARKIEWICZ, P. K. & ROTUNNO, R. 1989 Low Froude number flow past three-dimensional obstacles. Part I: baroclinically generated lee vortices. *J. Atmos. Sci.* **46**, 1154–1164.
- SNYDER, W. H., THOMPSON, R. S., ESKRIDGE, R. E., LAWSON, R. E., CASTRO, I. P., LEE, J. T., HUNT, J. C. R. & OGAWA, Y. 1985 The structure of strongly stratified flow over hills: dividing streamline concept. *J. Fluid Mech.* **152**, 249–288.
- THOMPSON, R. S. & SNYDER, W. H. 1976 EPA Fluid Modeling Facility, *Proc. Conf. on Environ. Modeling and Simulation, Cincinnati, USEPA Rep.* EPA-600/9-76-016, Washington, D.C.
- WONG, K. K. & KAO, T. W. 1970 Stratified flow over extended obstacles and its application to topographical effect on vertical wind shear. *J. Atmos. Sci.* **27**, 884–889.